Supplementary material for

High-pressure phase transition and equation of state of hydrous Al-bearing silica

Giacomo Criniti[1,*], Takayuki Ishii[2], Alexander Kurnosov[1], Konstantin Glazyrin[3], Tiziana Boffa Ballaran[1]

1 Bayerisches Geoinstitut, Universität Bayreuth, 95440 Bayreuth, Germany

2 Center for High Pressure Science and Technology Advanced Research, 100094 Beijing, China

3 Deutsches Elektronen-Synchrotron DESY, Notkestr. 85, 22603 Hamburg, Germany

* corresponding author: giacomo.criniti@uni-bayreuth.de

Table S1. Details for the high-pressure experiments performed in this study.

Label	Sample(s)	Culet (μm)	Pressure medium	*P* range (GPa)	Technique
DACX	Al5, Al11	350	He	0-50.13(4)	XRD
DAC1	Al5	400	Ne	0-10.9(1)	Raman
DAC2	Al5	400	He	0-9.4(1)	Raman
DAC3	Al5	400	He	0-38.2(1)	Raman
DAC4	Al11	250	He	0-44.30(3)	Raman

Table S2. Unit-cell lattice parameters of Al5 as a function of pressure. *P* is calculated as the average value between pressure measured before and after XRD measurements using the ruby fluorescence shift (Shen et al. 2020), and σ *P* is the semi-difference between the two values. Errors on the cell parameters represent one standard deviation.

P (GPa)	σ_P (GPa)	a (Å)	σ_a (Å)	b (Å)	σ_b (Å)	c (Å)	σ_c (Å)	V (Å³)	σ_V (Å³)
1.06	0.02	4.1940	0.0001			2.6714	0.0001	46.988	0.003
3.23	0.04	4.1813	0.0001			2.6679	0.0001	46.644	0.003
6.02	0.02	4.1667	0.0001			2.6634	0.0001	46.239	0.003
7.86	0.02	4.1573	0.0001			2.6603	0.0001	45.979	0.003
9.13	0.02	4.1515	0.0001			2.6580	0.0001	45.810	0.003
10.78	0.02	4.1440	0.0002			2.6554	0.0001	45.599	0.003
12.33	0.02	4.1374	0.0001			2.6524	0.0001	45.403	0.003
13.86	0.03	4.1311	0.0002			2.6498	0.0001	45.222	0.003
16.09	0.02	4.1309	0.0003	4.1125	0.0003	2.6459	0.0001	44.949	0.005
17.32	0.03	4.1275	0.0002	4.1045	0.0003	2.6438	0.0001	44.789	0.005
19.10	0.04	4.1237	0.0002	4.0902	0.0003	2.6413	0.0001	44.550	0.005
20.30	0.03	4.1187	0.0002	4.0863	0.0003	2.6392	0.0001	44.418	0.005
21.75	0.03	4.1173	0.0002	4.0718	0.0004	2.6368	0.0001	44.205	0.005
23.57	0.07	4.1135	0.0002	4.0597	0.0004	2.6338	0.0001	43.983	0.005
25.56	0.03	4.1094	0.0002	4.0470	0.0004	2.6305	0.0001	43.747	0.005
28.02	0.05	4.1040	0.0002	4.0345	0.0004	2.6259	0.0001	43.479	0.005
29.00	0.02	4.1019	0.0002	4.0280	0.0003	2.6245	0.0001	43.364	0.004
30.51	0.03	4.0985	0.0002	4.0200	0.0003	2.6212	0.0001	43.185	0.004
32.21	0.04	4.0946	0.0002	4.0106	0.0003	2.6178	0.0001	42.989	0.004
33.79	0.03	4.0910	0.0002	4.0031	0.0003	2.6149	0.0001	42.824	0.004
35.72	0.04	4.0865	0.0002	3.9940	0.0003	2.6114	0.0001	42.622	0.004
38.02	0.04	4.0821	0.0002	3.9833	0.0003	2.6071	0.0001	42.391	0.004
40.04	0.03	4.0780	0.0002	3.9729	0.0003	2.6036	0.0001	42.183	0.004
41.87	0.03	4.0751	0.0002	3.9646	0.0003	2.6001	0.0001	42.007	0.004
43.83	0.02	4.0714	0.0002	3.9552	0.0003	2.5968	0.0001	41.816	0.004
45.69	0.03	4.0680	0.0002	3.9469	0.0003	2.5938	0.0001	41.645	0.004
48.21	0.04	4.0650	0.0002	3.9363	0.0003	2.5889	0.0001	41.425	0.004
50.13	0.04	4.0610	0.0002	3.9268	0.0003	2.5856	0.0001	41.232	0.004

Table S3. Unit-cell lattice parameters of Al11 as a function of pressure. *P* is calculated as the average value between pressure measured before and after XRD measurements using the ruby fluorescence shift (Shen et al., 2020), and σ *P* is the semi-difference between the two values. Errors on the cell parameters represent one standard deviation.

P (GPa)	σ$_P$ (GPa)	*a* (Å)	σ$_a$ (Å)	*b* (Å)	σ$_b$ (Å)	*c* (Å)	σ$_c$ (Å)	*V* (Å^3)	σ$_V$ (Å^3)
1.06	0.02	4.2500	0.0002	4.1762	0.0003	2.6799	0.0001	47.566	0.004
3.23	0.04	4.2380	0.0002	4.1606	0.0002	2.6766	0.0001	47.196	0.004
6.02	0.02	4.2241	0.0002	4.1424	0.0002	2.6718	0.0001	46.752	0.004
7.86	0.02	4.2154	0.0002	4.1313	0.0002	2.6684	0.0001	46.470	0.004
9.13	0.02	4.2106	0.0002	4.1220	0.0002	2.6663	0.0001	46.277	0.004
10.78	0.02	4.2039	0.0002	4.1126	0.0002	2.6632	0.0001	46.043	0.003
12.33	0.02	4.1979	0.0002	4.1036	0.0002	2.6608	0.0001	45.837	0.004
13.86	0.03	4.1923	0.0002	4.0949	0.0002	2.6576	0.0001	45.623	0.003
16.09	0.02	4.1838	0.0002	4.0820	0.0002	2.6535	0.0001	45.317	0.003
17.32	0.03	4.1801	0.0002	4.0751	0.0002	2.6511	0.0001	45.160	0.004
19.10	0.04	4.1750	0.0002	4.0647	0.0002	2.6482	0.0001	44.941	0.003
20.30	0.03	4.1708	0.0002	4.0588	0.0002	2.6461	0.0001	44.795	0.003
21.75	0.03	4.1667	0.0002	4.0501	0.0002	2.6433	0.0001	44.607	0.004
23.57	0.07	4.1610	0.0002	4.0415	0.0002	2.6398	0.0001	44.391	0.003
25.56	0.03	4.1548	0.0002	4.0314	0.0002	2.6360	0.0001	44.152	0.003
28.02	0.05	4.1483	0.0002	4.0190	0.0002	2.6319	0.0001	43.879	0.003
29.00	0.02	4.1440	0.0002	4.0138	0.0002	2.6294	0.0001	43.734	0.004
30.51	0.03	4.1399	0.0002	4.0067	0.0002	2.6268	0.0001	43.572	0.003
32.21	0.04	4.1358	0.0002	3.9987	0.0002	2.6236	0.0001	43.389	0.003
33.79	0.03	4.1316	0.0002	3.9915	0.0002	2.6207	0.0001	43.219	0.003
35.72	0.04	4.1265	0.0002	3.9828	0.0002	2.6172	0.0001	43.014	0.003
38.02	0.04	4.1209	0.0002	3.9726	0.0002	2.6132	0.0001	42.780	0.003
40.04	0.03	4.1162	0.0002	3.9638	0.0001	2.6095	0.0001	42.575	0.003
41.87	0.03	4.1118	0.0002	3.9564	0.0001	2.6063	0.0001	42.399	0.003
43.83	0.02	4.1073	0.0002	3.9485	0.0002	2.6028	0.0001	42.210	0.003
45.69	0.03	4.1034	0.0002	3.9409	0.0002	2.5994	0.0001	42.034	0.003
48.21	0.04	4.098	0.0002	3.9315	0.0002	2.5949	0.0001	41.806	0.003
50.13	0.04	4.0938	0.0002	3.9239	0.0002	2.5916	0.0001	41.631	0.003

Table S4. Observed Raman shifts of B_{1g} (stishovite) and A_g (CaCl$_2$-type phase) optic modes of Al5 (DAC1, DAC2, DAC3) as a function of pressure. Error on the peak position represent one standard deviation. P is calculated as the average value between pressure measured before and after Raman spectroscopy measurements using the ruby fluorescence shift (Shen et al. 2020), and σP is the semi-difference between the two values. Asterisks next to P values indicate measurements performed during decompression.

P (GPa)	σP (GPa)	ω (cm^{-1})	$\sigma \omega$ (cm^{-1})
DAC1			
0		224.99	0.09
1.3	0.1	224.01	0.07
3.5	0.1	220.86	0.04
5.4	0.1	220.24	0.11
6.6	0.1	218.67	0.06
7.7	0.1	217.91	0.07
9.7	0.2	216.3	0.04
10.9	0.1	216.42	0.09
9.6*	0.1	216.71	0.15
4.1*	0.1	220.71	0.05
DAC2			
0		224.49	0.06
4.0	0.2	221.57	0.08
6.6	0.1	219.01	0.05
9.4	0.1	217.75	0.06
DAC3			
0		225.18	0.03
3.4	0.1	221.69	0.06
6.7	0.1	219.05	0.04
9.7	0.1	216.81	0.04
11.0	0.1	215.05	0.05
13.6	0.1	212.59	0.05
14.8	0.1	211.63	0.1
17.4	0.1	209.66	0.05
18.65	0.1	208.64	0.12
20.3	0.2	207.17	0.05
21.4	0.1	206.73	0.06
22.5	0.1	206.47	0.08
24.1	0.1	205.71	0.06
24.7	0.1	204.34	0.08
25.6	0.1	205.95	0.19
26.9	0.1	206.41	0.11
28.5	0.1	206.57	0.11
29.6	0.1	205.05	0.11
31.2	0.1	206.96	0.15
33.0	0.2	210.7	0.3

34.9	0.1	207.86	0.06
36.3	0.2	212.15	0.06
38.2	0.2	213.92	0.07
26.7*	0.2	206.73	0.08

Table S5. Observed Raman shifts of the A_g (CaCl$_2$-type phase) optic mode of Al11 (DAC4) as a function of pressure. Error on the peak position represent one standard deviation. P is calculated as the average value between pressure measured before and after Raman spectroscopy measurements using the ruby fluorescence shift (Shen et al. 2020), and σP is the semi-difference between the two values. Asterisks next to P values indicate measurements performed during decompression.

P (GPa)	σP (GPa)	ω (cm^{-1})	σ_ω (cm^{-1})
		DAC4	
0		226.91	0.03
0.14	0.02	226.39	0.06
0.38	0.02	225.99	0.05
1.45	0.10	225.44	0.04
2.22	0.03	225.57	0.04
2.79	0.03	225.53	0.04
3.24	0.02	225.25	0.03
3.48	0.02	225.84	0.07
3.48	0.02	226.00	0.05
4.23	0.02	224.64	0.05
5.22	0.02	224.73	0.03
5.65	0.02	224.66	0.04
6.28	0.02	224.52	0.04
7.10	0.02	224.29	0.03
7.10	0.02	223.76	0.03
8.16	0.03	224.10	0.03
8.79	0.02	224.16	0.03
9.43	0.05	224.05	0.03
15.97	0.03	223.66	0.03
17.17	0.06	222.91	0.02
24.60	0.10	225.80	0.05
26.87	0.11	231.18	0.34
28.24	0.07	235.32	0.31
32.17	0.02	244.46	0.14
36.69	0.07	250.32	0.21
41.65	0.09	262.70	0.10
44.30	0.03	265.31	0.14
43.74*	0.02	262.56	0.13
42.95*	0.02	262.69	0.09
40.44*	0.02	253.05	0.16
35.50*	0.03	249.00	0.09
32.9*	0.2	241.32	0.19
25.0*	0.5	225.98	0.08
22.2*	0.8	224.55	0.06
20.7*	0.5	224.41	0.05

Table S6. Fractional atomic coordinates of oxygen and symmetry breaking mode $\Gamma2+$ as a function of pressure. P is calculated as the average value between pressure measured before and after XRD measurements, and σP is the semi-difference between the two values. Errors on the fractional atomic coordinates represent one standard deviation.

| P	σ_P	$x(O)$	$\sigma_{x(O)}$	$y(O)$	$\sigma_{y(O)}$	$\Gamma2+$
1.06	0.02	0.3059	0.0003			0
3.23	0.04	0.3056	0.0003			0
6.02	0.02	0.3053	0.0003			0
7.86	0.02	0.3052	0.0002			0
9.13	0.02	0.3051	0.0003			0
10.78	0.02	0.3052	0.0002			0
12.33	0.02	0.3054	0.0002			0
13.86	0.03	0.3054	0.0002			0
16.09	0.02	0.3056	0.0003	0.6977	0.0006	0.0192
19.10	0.04	0.3081	0.0004	0.7007	0.0004	0.0215
21.75	0.03	0.3091	0.0005	0.6999	0.0011	0.0522
25.56	0.03	0.3111	0.0003	0.7034	0.0007	0.0839
28.02	0.05	0.3115	0.0004	0.7049	0.0008	0.0947
29.00	0.02	0.3122	0.0004	0.7045	0.0008	0.0963
30.51	0.03	0.3126	0.0003	0.7161	0.0007	0.1078
32.21	0.04	0.3125	0.0009	0.7055	0.0021	0.1019
33.79	0.03	0.3137	0.0004	0.7079	0.0007	0.1242
35.72	0.04	0.3142	0.0003	0.7085	0.0006	0.1303
38.02	0.04	0.3149	0.0003	0.7094	0.0006	0.1393
40.04	0.03	0.3158	0.0003	0.7104	0.0006	0.1506
41.87	0.03	0.3162	0.0002	0.7116	0.0005	0.159
43.83	0.02	0.3168	0.0003	0.7118	0.0006	0.1634
45.69	0.03	0.3171	0.0003	0.7135	0.0007	0.174
48.21	0.04	0.3184	0.0003	0.7145	0.0007	0.1875
50.13	0.04	0.3187	0.0003	0.7150	0.0006	0.1918
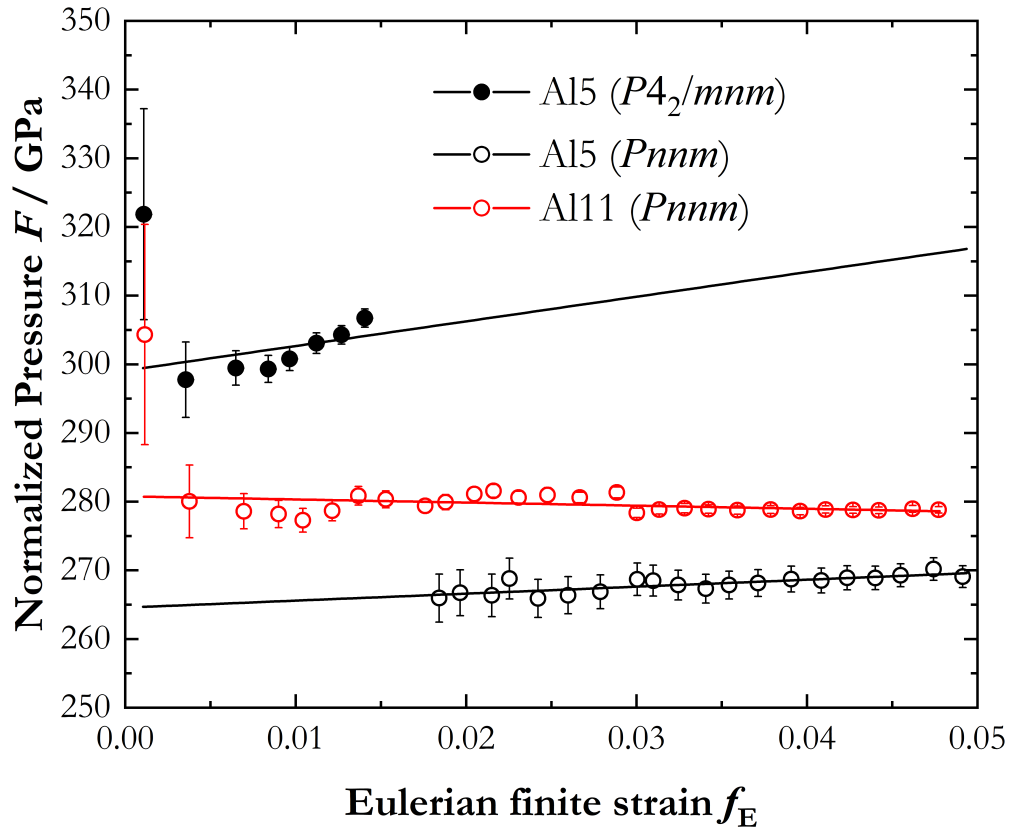
Figure S1. f_E-F plot of the EOSs of Al5 ($P42/mnm$ and $Pnnm$) and Al11 ($Pnnm$). The normalized pressure F was calculated as $F = P/[3f_E (2f_E +1)^{5/2})$, where $f_E = [(V_0/V)^{2/3}-1]/2$ is the Eulerian finite strain. Note that K'_{T0} of tetragonal Al5 was fixed to 4.8 in the fitting procedure (see main text for details).
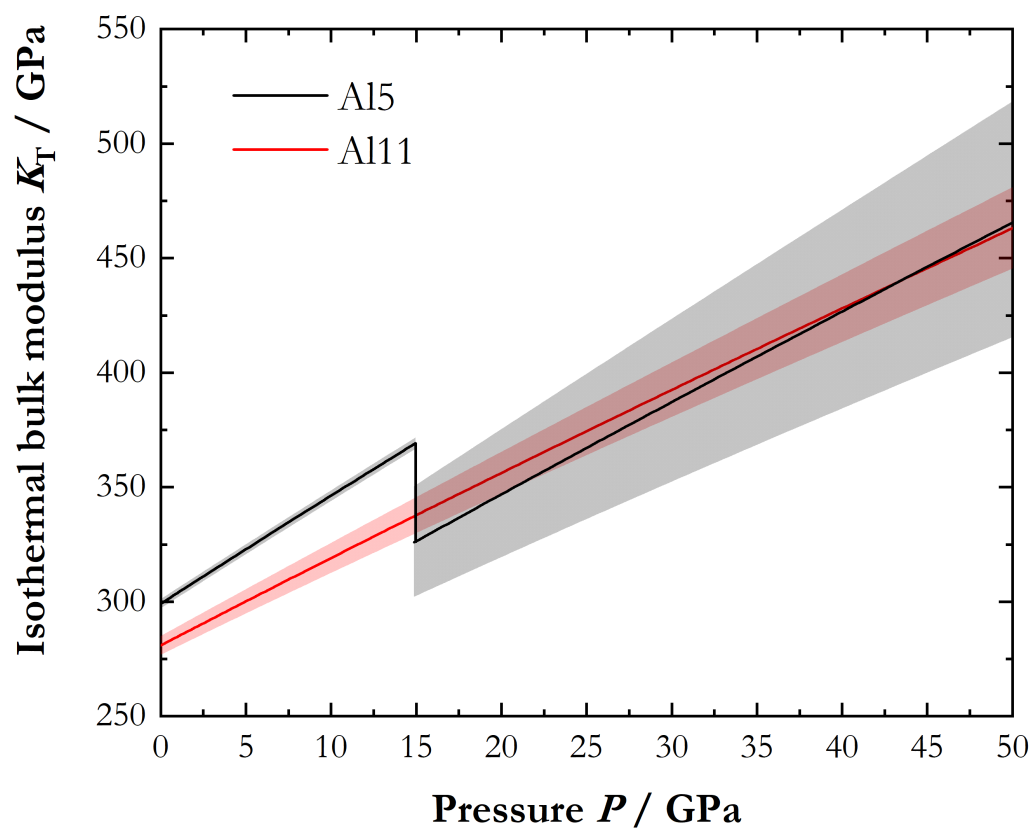
Figure S2. Pressure evolution of the isothermal bulk modulus K_T of Al5 (black) and Al11 (red) samples investigated in this study. At about 16 GPa, a phase transition from tetragonal to orthorhombic occurs in Al5 and causes a drop in K_T. Shaded area represent propagated uncertainties.
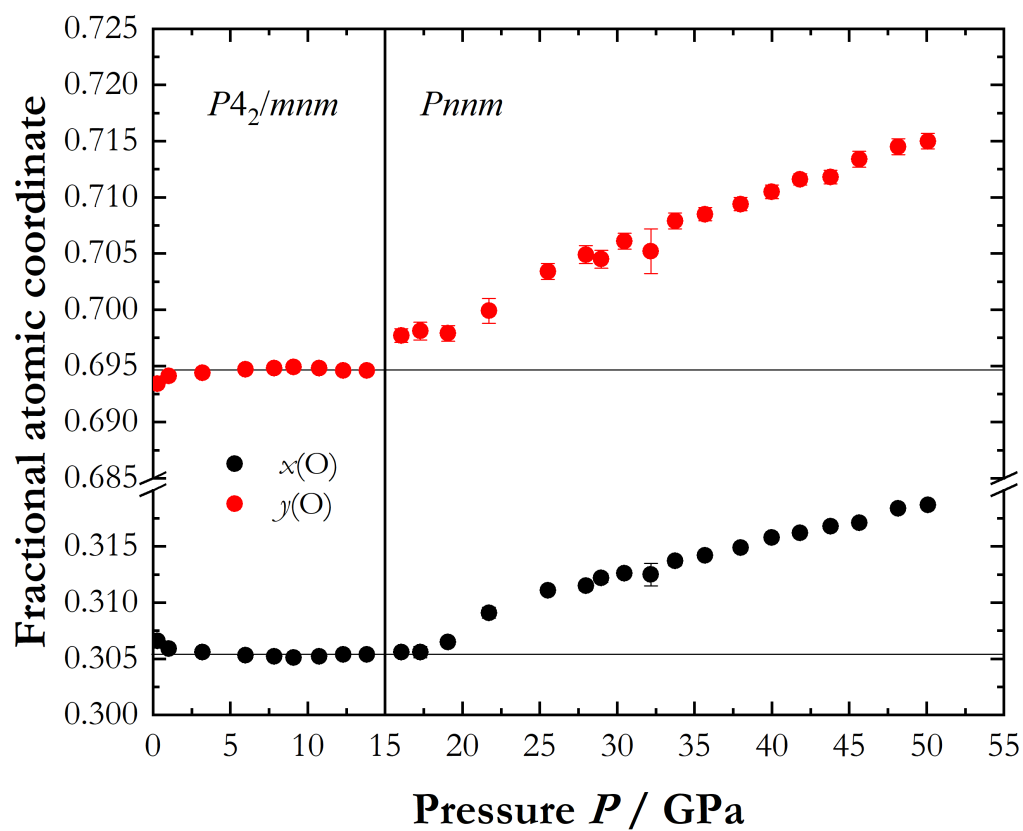
Figure S3. Fractional *x* and *y* coordinates of O in the tetragonal ($P4_2/mnm$) and orthorhombic

(*Pnnm*) phases of Al5 as a function of pressure. Horizontal lines represent values of *x*(O) and

y(O) = 1- *x*(O)assumed for the tetragonal phase in the stability field of the orthorhombic phase,

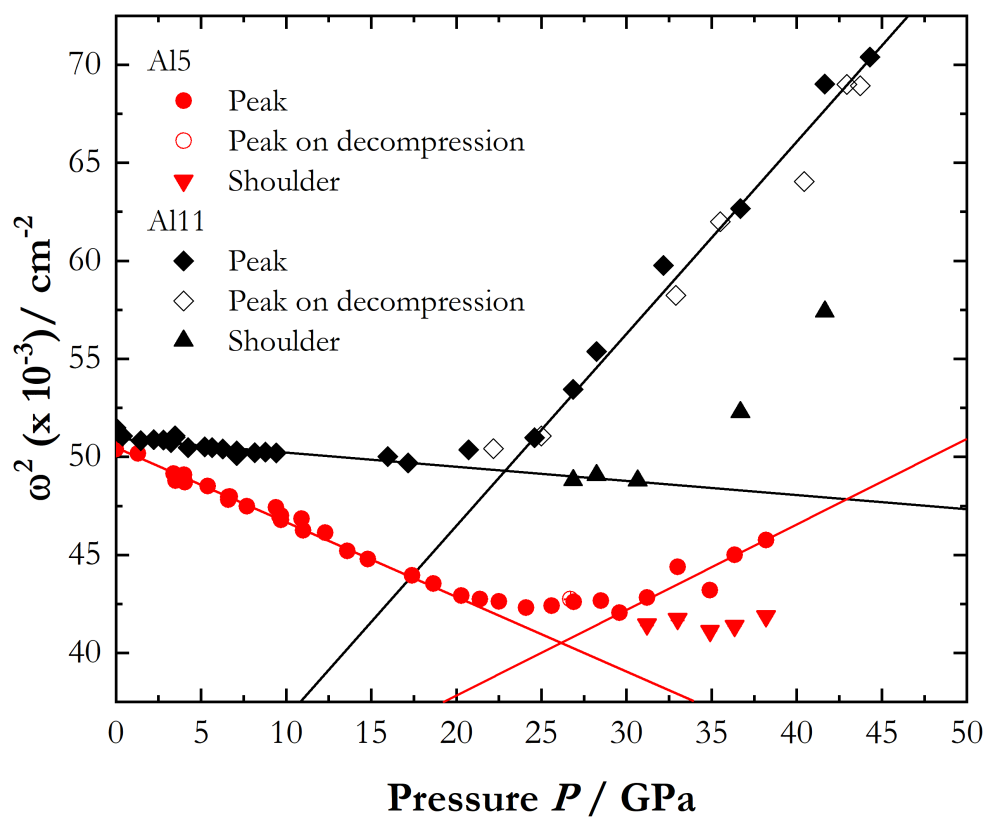which are required in the symmetry-mode decomposition analysis.

Figure S4. Pressure evolution of Raman bands and their shoulders in Al5 and Al11. Empty symbols represent points collected upon decompression. The shoulder at lower wavenumber represented by black (Al11) and red (Al5) triangles is less intense and tend to disappear as pressure increases.